



RF design optimization for the SHINE 3.9 GHz cavity

Yu-Xin Zhang^{1,2} · Jin-Fang Chen^{1,3} · Dong Wang^{1,3}

Received: 2 January 2020 / Revised: 17 April 2020 / Accepted: 21 April 2020 / Published online: 5 July 2020
© China Science Publishing & Media Ltd. (Science Press), Shanghai Institute of Applied Physics, the Chinese Academy of Sciences, Chinese Nuclear Society and Springer Nature Singapore Pte Ltd. 2020

Abstract The Shanghai high-repetition-rate XFEL and extreme light facility (SHINE) under construction is designed to be one of the most advanced free electron laser (FEL) facilities in the world. The main part of the SHINE facility is an 8 GeV superconducting Linac operating in continuous wave (CW) mode. The Linac consists of seventy-five 1.3 GHz and two 3.9 GHz cryomodules. Based on the design and experience of 3.9 GHz cavities in the European X-ray free electron laser (E-XFEL) and the Linac coherent light source-II (LCLS-II) projects, we optimize the SHINE 3.9 GHz cavity design to adapt it for CW mode operation. In this paper, we present a particular redesign of the end group for the SHINE 3.9 GHz superconducting cavity that includes a redesign of the end cell and beam pipe to shift away the potentially troublesome lowest high-order modes (HOMs), a modification of the main coupler antenna, and a tuning of the HOM notch filter to meet the cavity requirements. RF losses calculations on the HOM coupler antennas show that the overheating on the inner

conductor at the operating mode is diminished significantly. Furthermore, we have also studied the HOMs to ensure there are no dangerously trapped modes in the optimized cavity design.

Keywords Superconducting cavity · Higher-order modes · RF design · 3.9 GHz

1 Introduction

Building upon experience in both traditional and newly developed superconducting technology for particle accelerators, the Shanghai high-repetition-rate XFEL and extreme light facility (SHINE) project is expected to be one of the most advanced high-repetition-rate X-ray FEL facilities in the world [1–3]. The facility will provide hard coherent X-ray radiation over a broad spectrum for basic research in various fields, including biology, nonlinear physics, and material science. The SHINE Linac is equipped with seventy-five 1.3 GHz and two 3.9 GHz cryomodules. The third harmonic section compensates the nonlinear longitudinal phase space distortion due to the accelerating field curvature in the 1.3 GHz TESLA cavities prior to bunch compression [4, 5]. This allows the delivery of high current beams with sufficiently low emittance for the production of 0.4 to 25 keV FEL light to the experimental users. The 3.9 GHz cryomodules are installed after the first acceleration section and before the first bunch compressor, as shown in Fig. 1. Each 3.9 GHz cryomodule includes eight 9-cell elliptical cavities at 3.9 GHz and a quadruple magnet package. The requirements for the 3.9 GHz cryomodule and cavity in the SHINE Linac are shown in Table 1 [6].

This work was partially supported by the National Key Research and Development Program of China (No. 2016YFA0401900) and the Shanghai Municipal Science and Technology Major Project (No. 2017SHZDZX02).

✉ Jin-Fang Chen
chenjinfang@zjlab.org.cn

Yu-Xin Zhang
zhangyuxin@sinap.ac.cn

¹ Shanghai Institute of Applied Physics, Chinese Academy of Sciences, Shanghai 201204, China

² ShanghaiTech University, Shanghai 201210, China

³ Shanghai Advanced Research Institute, Chinese Academy of Sciences, Shanghai 201204, China

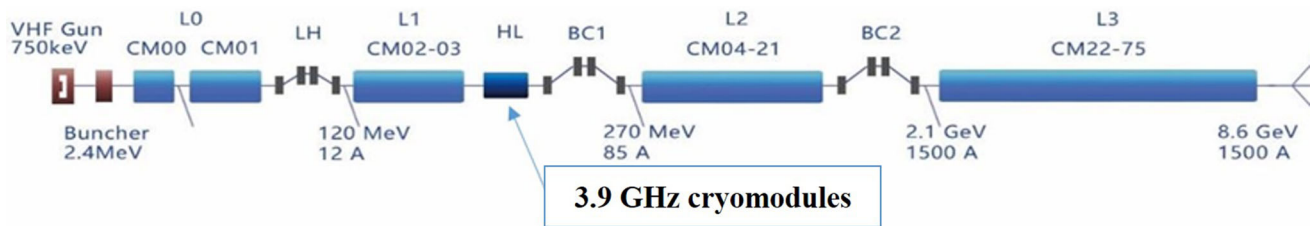


Fig. 1 (Color online) SHINE Linac layout

Table 1 The requirements for the 3.9 GHz cryomodule and cavity in SHINE Linac

Requirements	Nominal	Max
Beam to RF phase	-153°	
Number of active cavities	15	16
Cavity Q_0	2.0×10^9	
Operating gradient with 15 cavities	13.1 MV/m	15.0 MV/m
HOM Q_{ext}	$<1 \times 10^6$	

Compared to the mature 1.3 GHz TESLA cavity, the 3.9 GHz cavity is relatively less mature and the geometry is evolving over different projects. The first 3.9 GHz SRF cavity was proposed by DESY in 2002 for the FLASH VUV facility [7, 8] and further optimized by Fermi National Accelerator Laboratory (FNAL) for FLASH. Based on the FLASH 3.9 GHz cavity, INFN-LASA made several mechanical modifications to facilitate production and put the resulting cavity into use in the E-XFEL machine, in which the cavity witnessed its first beam in 2017 [9, 10]. FNAL subsequently reduced the beam pipe size using a tapered transition and shortened the HOM antenna length to adapt the cavity for CW operation in LCLS-II [11]. Based on the above experiences, we optimized the RF design for the SHINE 3.9 GHz cavity. Differing from the modifications for LCLS-II, we modified not only the beam pipe and accessories, but also the shape of the end half-cell.

2 Motivation of design optimization

We made some targeted modifications to meet the needs of the SHINE project, based on the previous studies and some measurement results on the prototypical and series 3.9 GHz cavities for E-XFEL at INFN-LASA. During the measurements, it was found that in some cavities, the lowest dipole modes could be shifted down to close to 3.9 GHz after fabrication and chemical treatments, which may lead to difficulties for π -mode operation and notch tuning in the HOM coupler band stop filter [12, 13].

Consequently, the resultant power leakage through the HOM couplers at operating frequency may become considerable. Therefore, it is necessary to optimize the cavity geometry. Simulations show that the lowest dipole mode is located at the region of the end cell, main coupler, and beam pipe (PEC boundary), as shown in Fig. 2. Hence, its frequency can be efficiently shifted up by squeezing the end-cell wall, or by reducing the beam pipe diameter or main coupler port size. Keeping the end cell unchanged from the E-XFEL 3.9 GHz cavity shape, the LCLS-II design shifts the lowest dipole modes up by 100 MHz by reducing the beam pipe diameter from 40 mm to 38 mm with a tapered transition.

Additionally, previous vertical tests showed a thermal quench of the HOM coupler antenna at around 20 MV/m in CW mode for the FLASH and E-XFEL cavity designs [14] in which the 3.9 GHz cavity nominally operates in pulse mode. In high-repetition-rate machines, such as LCLS-II and SHINE, the cavity will operate in CW mode, which results in higher heat loads. To reduce the risk of cavity quench caused by the HOM antennas, some modifications on the HOM coupler antennas are necessary to adapt them for CW operation.

In this paper, we present our particular modifications on the end group of the 3.9 GHz cavity for SHINE, including a redesigned end cell and beam pipe, an adjustment of the main coupler antenna, and a tuning of the HOM notch.

3 Redesign of end group

To shift the potentially dangerous lowest dipole modes, we redesigned the end half-cell with an iris diameter of 38 mm and a straight beam pipe of the same size. Figure 3

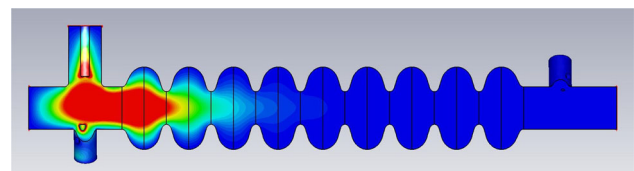


Fig. 2 (Color online) The electric field distribution of the lowest dipole mode in the SHINE 3.9 GHz cavity

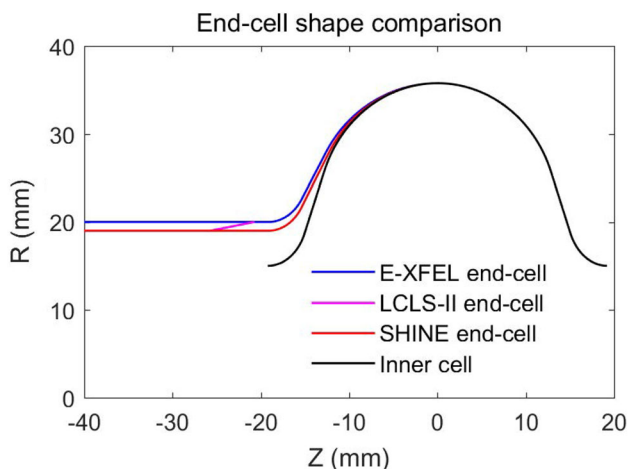


Fig. 3 (Color online) End-cell shape of 3.9 GHz cavity for SHINE, E-XFEL, and LCLS-II

shows the end-group shape of the SHINE 3.9 GHz cavity and compares it to the ones in the E-XFEL and LCLS-II projects. In detail, compared to E-XFEL, we reduced the diameter of the beam tube from 40 mm to 38 mm; compared to LCLS-II, we removed the tapered transition. This modification gives a simpler geometry that is expected to be beneficial to cavity fabrication and surface processing.

The cavity shape was designed using the SUPERFISH [15] and BUILDCAVITY codes [16, 17]. Table 2 shows the geometric parameters of the 3.9 GHz cavity for SHINE and a comparison to the other two projects. The parameters describing a half-cell are shown in Fig. 4. In the end-cell redesign, only two parameters were modified, i.e., the iris radius (R_{ir}) and the horizontal axis length of the equatorial ellipse (A).

In the cavity design for SHINE, the frequency and field flatness were adjusted by A . We reached the goal frequency and achieved a flat field distribution in the nine cells by setting A at 14 mm. The field flatness of the SHINE 3.9

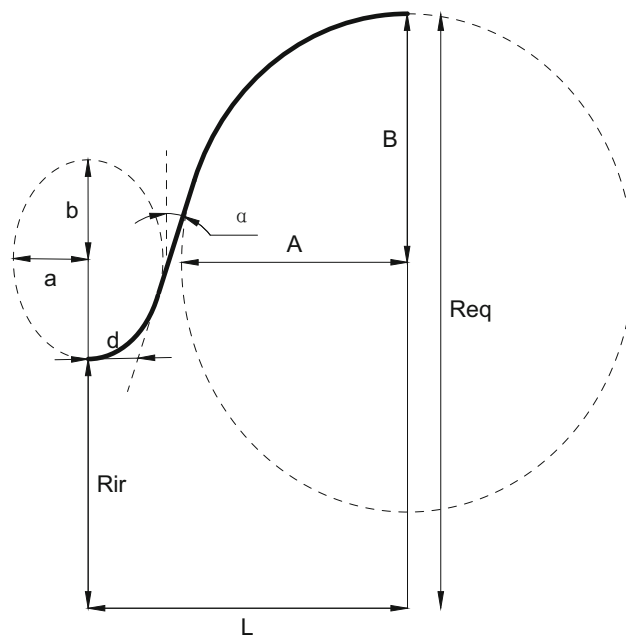


Fig. 4 Parameters describing a half-cell

GHz cavity after modification is shown in Fig. 5, in which the accelerating gradient is normalized to 1 MV/m.

Table 3 shows the main RF parameters of the SHINE 3.9 GHz cavity design and a comparison with the parameters in E-XFEL and LCLS-II. Most of the RF parameters are the same, except for the R/Q and the lowest dipole mode frequency. Owing to the smaller iris diameter in the end half-cell, we achieved a slightly higher R/Q and pushed the lowest dipole modes to 4165 MHz, which is 265 MHz higher than the operating frequency. The electric field distribution of the lowest dipole mode is shown in Fig. 2. This larger frequency distance would be sufficient to avoid the downshift of the accelerating mode frequency during the fabrication stage.

Table 2 Geometric parameters of 3.9 GHz cavity for SHINE and a comparison

Parameters (mm)	Inner cell	End cell (E-XFEL, LCLS-II)	End cell (SHINE)
R_{ir} (mm)	15	20	19
L (mm)	19.22	19.12	19.12
R_{eq} (mm)	35.79	35.79	35.79
A (mm)	13.6	14.4	14
B (mm)	15	15	15
a (mm)	4.5	4.5	4.5
b (mm)	6	6	6
d (mm)	3	2.4	2.4
α (°)	17.5	27.3	26.5
D_{bp} (mm)	30	40, 40 → 38	38
L_{bp} (mm)		80.11	80.11

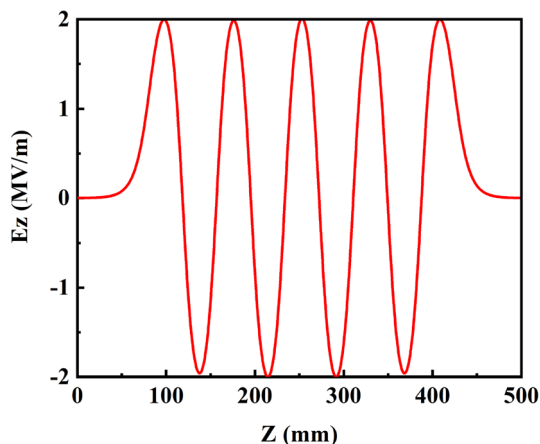


Fig. 5 Field flatness of SHINE 3.9 GHz cavity after modification

4 Coupler modification

The 3.9 GHz cavity includes four couplers comprising a fundamental power coupler (FPC), two HOM couplers, and a pick-up probe. Based on the redesign of the end cell and beam pipe, all the couplers need to be modified to meet the requirements of SHINE. In particular, as mentioned above, the HOM coupler antennas need to be optimized to avoid overheating from CW operation. LCLS-II modified the HOM F-part and antenna tip [11] to shift the tip away from the strong magnetic field region and reduce the surface area of the antenna exposed to the magnetic field. For SHINE, we adopted the same idea as LCLS-II in modifying the HOM coupler and calculated the RF losses on the HOM coupler antennas.

4.1 Main coupler antenna adjustment

The FPC in the SHINE 3.9 GHz cavity is a coaxial coupler that transmits the RF power into the cavity. Similar to E-XFEL and LCLS-II, we adopted a hollow inner conductor to reduce its weight. Owing to the modification of the end group, the length of the FPC antenna has to be adjusted to meet the external Q (Q_{ext}) requirement of

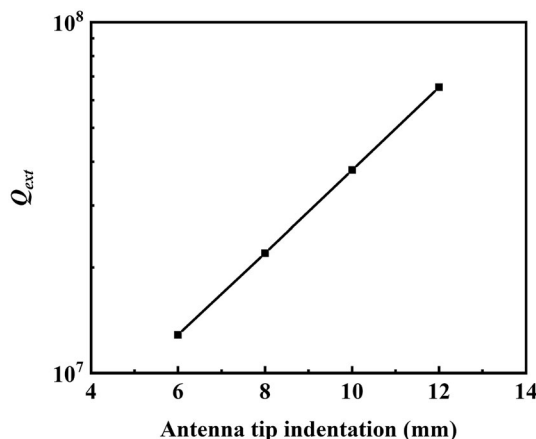


Fig. 6 The relationship between Q_{ext} and FPC antenna tip indentation

SHINE. The optimum Q_{ext} is calculated from Eqs. (1) and (2) [18]:

$$\beta_{opt} = \left[\left(1 + \frac{I_b Q_0 (R/Q) \cos \varphi_s}{V_c} \right)^2 + \left(\frac{2Q_0 \delta f_m}{f_0} \right)^2 \right]^{1/2}, \tag{1}$$

$$Q_{ext} = Q_0 / \beta_{opt}. \tag{2}$$

For the SHINE 3.9 GHz cavity, using the nominal parameters in Table 1, the cavity RF parameters in Table 3, and the maximum average beam current of 0.3 mA, we obtained the optimum $Q_{ext} = 2.2 \times 10^7$ without microphonics detuning, and $Q_{ext} = 2.1 \times 10^7$ with a maximum estimated microphonics detuning of $\delta f_m = 30$ Hz. The microphonics will be compensated by a piezo-assisted tuner to minimize the peak detuning [19].

The target Q_{ext} was achieved by choosing a proper antenna length. Figure 6 shows the relationship between Q_{ext} and the distance from the antenna tip to the inner wall of the beam pipe. In order to ensure HOM safety, we used the conservative value of $Q_{ext} = 2.2 \times 10^7$ for the FPC. Therefore, an indentation of 8.0 mm was chosen for the FPC antenna tip in this paper, as indicated in Fig. 7.

Table 3 Main RF parameters of SHINE 3.9 GHz cavity and a comparison

Parameters	E-XFEL	LCLS-II	SHINE
Frequency (MHz)	3900	3900	3900
Number of cells	9	9	9
Active length, L_{cav} (m)	0.346	0.346	0.346
R/Q (Ω)	748	751	758
G (Ω)	277	275	276
E_{pk}/E_{acc}	2.3	2.3	2.3
B_{pk}/E_{acc} (mT/(MV/m))	4.9	4.9	4.9
Lowest dipole mode frequency (MHz)	3992	4092	4165

4.2 HOM coupler tuning

The HOM couplers in the 3.9 GHz cavity are of the coaxial type and have two basic functions: 1) rejecting the fundamental mode and 2) extracting the HOM energy over a broad frequency band. The rejection of the accelerating mode can be fulfilled by tuning the HOM notch filter, as illustrated in Fig. 8a. We simulated the S parameters between the 4 coupler ports with CST Microwave Studio [20], as shown in Fig. 8b. Figure 9a shows the transmitted signals from the FPC port to the pick-up and from the pick-up to HOM1 (port 2). The notch position for HOM coupler 1 (port 2) is shown in Fig. 9b. Similarly, the notch frequency of HOM coupler 2 (port 3) was tuned the same way. The tuning sensitivity of the HOM notch filter around the goal frequency is about 0.24 MHz/ μm .

Usually, the tuning of the cavity HOM notch filter is completed at room temperature before the vertical test. A slight deviation from the goal notch frequency is common due to the tuning precision limit. We used the S parameter, which is defined in Eq. (3), to calculate the average RF power leak of the fundamental mode through a HOM coupler, as shown in Fig. 9c. Using 1 W as a reference, the HOM notch frequency of SHINE 3.9 GHz cavity should be tuned to within ± 8 MHz from the goal frequency.

$$S_{24} - S_{14} = 10 \lg \frac{P_2}{P_4} - 10 \lg \frac{P_1}{P_4} = 10 \lg \frac{P_2}{P_1} \text{ (dB)} \quad (3)$$

where $S_{24} - S_{14}$ is calculated in Fig. 9b, $P_1 = \frac{(E_{\text{acc}} \times L_{\text{cav}})^2}{R/Q \cdot Q_{\text{ext}}}$ is the output power from port 1, P_2 is the radiation power from HOM coupler 1 (port 2), and P_4 is the input power to port 4.

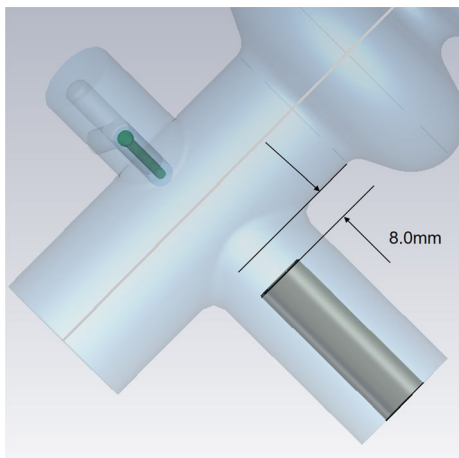


Fig. 7 (Color online) Antenna indentation of the main coupler

4.3 RF losses on HOM antenna

Due to poor cooling of the HOM antenna inner conductor, heating of the niobium antenna tip by the magnetic field may lead to quench at high accelerating gradients, especially in CW mode operation. Figure 10 shows the geometry of the F-part and antenna in the 3.9 GHz HOM coupler. The RF losses can be expressed by Eq. (4). We calculated the RF losses on the HOM antenna at the maximum operating gradient of 15 MV/m.

Table 4 shows the RF losses on the HOM antennas of the SHINE 3.9 GHz cavity as well as on the E-XFEL and LCLS-II antennas. The result shows that at the same accelerating gradient of 15 MV/m, the RF losses on the antenna for the SHINE cavity are lower than the other two and are around 3/4 of those for LCLS-II. Further, if the notch filter is not perfectly tuned but has a deviation within ± 8 MHz, the maximum change of the RF losses on the HOM antenna is less than 1%.

$$\text{RF losses} = \frac{1}{2} R_s \times \int |H|^2 dS. \quad (4)$$

5 Dangerous HOMs check

HOMs with high loaded quality factor, Q_L , may be coherently excited when beams pass through the cavity. Monopole HOMs may be excited when a bunch of charged particles passes through the axis of the cavity, while higher-pole HOMs may be excited if a number of charged particles traverse the cavity with an offset to the axis. The interaction of the HOM fields with the beams may deteriorate the beam quality in terms of the energy spread, emittance growth, or even beam stability. In addition, a significant HOM-induced power loss in the cavity will also add an extra heat load to the cryogenic system, which may lead a cost increase in building and operating the Linac.

Generally, most of the HOM power can be extracted out of the cavities through the HOM couplers, the FPC, and the beam pipes. The cutoff frequency of the lowest dipole modes in the 38 mm diameter beam pipe is about 4.6 GHz. Hence, the HOMs above 4.6 GHz can propagate through the beam pipes, and their power can also be extracted by the coupler ports on adjacent cavities, dissipated by the bellows between cavities, or even absorbed by the HOM absorbers located at both ends of the cryomodule. The dangerous HOMs in a cavity are those trapped inside the cavity with high Q_L , considerable R/Q , and frequencies close to the harmonics of the beam spectrum.

Because the end groups of the SHINE 3.9 GHz cavity have been redesigned with a smaller beam pipe diameter, it is necessary to confirm that no dangerously trapped HOMs

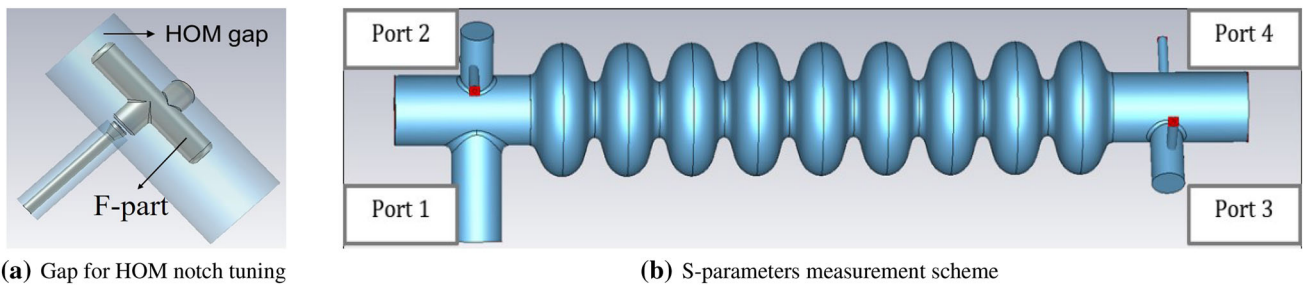
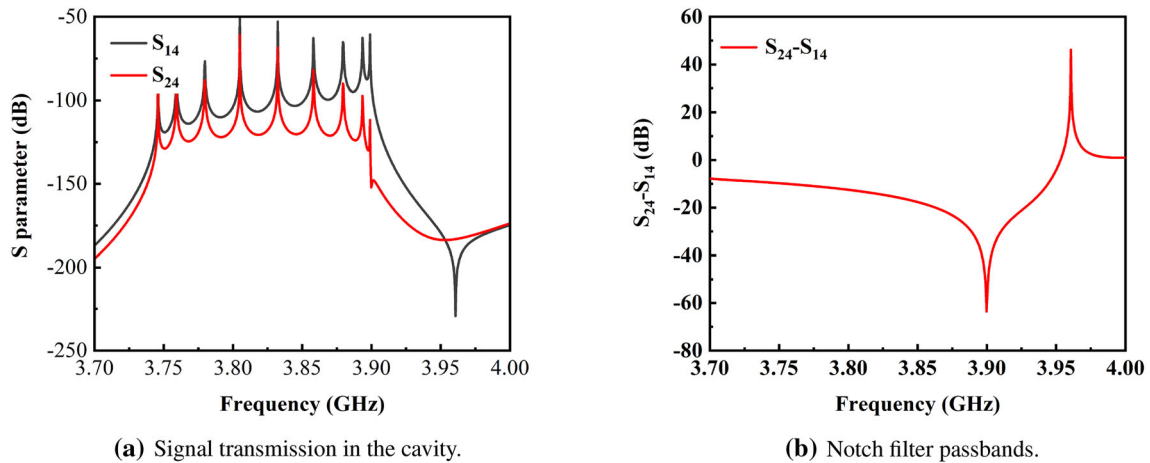
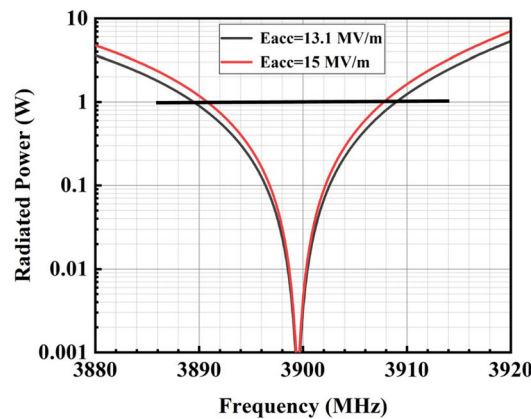


Fig. 8 (Color online) Notch filter tuning and measurement of SHINE 3.9 GHz cavity



(a) Signal transmission in the cavity.

(b) Notch filter passbands.



(c) Power radiation from one HOM coupler.

Fig. 9 (Color online) HOM coupler S parameter and power radiation

exist in the cavity. We have simulated the HOM eigenmodes up to 10 GHz with electric boundary conditions. Owing to the existence of hybrid modes, we do not specify the mode types. The Q_L , longitudinal, and transverse R/Q of all the modes are displayed in Fig. 11. The transverse R/Q was calculated with a radial off-set of 1 mm to the beam axis. We used the following definitions for the longitudinal and transverse shunt impedance [21]:

$$\left(\frac{R_{\parallel}}{Q}\right) = \frac{\left|\int_0^z [E_z(r, z)]_{r=0} e^{ikz} dz\right|^2}{\omega_0 W}, \tag{5}$$

$$\left(\frac{R_{\perp}}{Q}\right) = \frac{\left|\int_0^z \{\nabla_{\perp} [E_z(r, z)]\}_{r=r_0} e^{ikz} dz\right|^2}{\omega_0 W} \times \frac{1}{k^2}, \tag{6}$$

where $E_z(r, z)$ is the longitudinal component of the electric field along the beam trajectory, r is the radial offset, and W

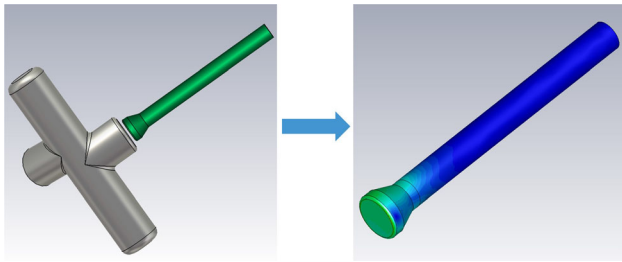


Fig. 10 (Color online) Surface for magnetic field integration on HOM antenna

Table 4 RF losses on HOM antenna

Parameter	E-XFEL	LCLS-II	SHINE
H_{pk} (A/m)	2381	1222	1033
S (mm ²)	249.04	231.45	231.45
RF loss/ R_s (A ²)	194.9	41.4	30.8

is the stored energy in the cavity. ω_0 is the resonant angular frequency, $k = \omega_0/c$, and $r_0 = 1$ mm.

A general case of HOM excitation can be expressed by Eqs. (7) and (8) [21], representing the HOM-induced maximum power loss and maximum transverse kick, respectively:

$$\langle P \rangle_{\max} = \frac{(R_{\parallel}/Q)\omega_0 q_0^2}{4t_b} \left(\frac{e^\alpha + 1}{e^\alpha - 1} \right), \tag{7}$$

$$|V_{\perp}|_{\max}^{r=r_0} = \frac{(R_{\perp}/Q)\omega_0 q_0 r_0 k}{4} \left(\frac{e^\alpha + 1}{e^\alpha - 1} \right), \tag{8}$$

where $\alpha = t_b/\tau$, t_b is the bunch spacing, $\tau = 2Q_L/\omega_0$ is the HOM signal decay time, and q_0 is the individual bunch charge. In the SHINE Linac, the minimum $t_b = 10^{-6}$ s, and the maximum bunch charge $q_0 = 300$ pC.

In general, SHINE requires the Q_L of each HOM to be less than 10^6 to ensure negligible power loss due to these

HOMs [6]. For the maximum repetition rate of 1 MHz, a HOM with $Q_L > 10^6$ leads to $t_b \ll \tau$, and the equations can be simplified to $\langle P \rangle_{\max} \approx (R_{\parallel}/Q)Q_L I_0^2$ and $V_{\perp} \approx I_0(R_{\perp}/Q)Q_L r_0 \omega_0/c$.

Using the maximum average beam current of 0.3 mA in the SHINE Linac, and $Q_0 = 2 \times 10^9$ for the 3.9 GHz cavity, the sum of the static and dynamic heat loads at the fundamental mode is about 20 W per cavity.

The maximum power loss calculated by equation 7 for all the modes (except accelerating mode) under 10 GHz is shown in the left picture of Fig. 12. The largest power loss appears at 7.33 GHz. Its E-field distribution is shown in Fig. 13a, from which we can see that it is not a trapped mode. Some other modes with $\langle P \rangle_{\max}$ at around 0.1 W, such as the one at 7.5 GHz that belongs to the second monopole passband, are similar to the modes in cavities with the same inner cells in E-XFEL and LCLS-II [22]. The maximum power loss of these modes is small compared with the fundamental mode. Therefore, we do not regard them to be dangerous in the cavity.

Similarly, we calculated the transverse voltages using Eq. (8) for all the modes (except accelerating mode) under 10 GHz in the SHINE 3.9 GHz cavity, as shown in the right picture of Fig. 12. One passband at around 9.6 GHz shows a relatively high transverse kick voltage with a maximum voltage of about 52 V. Because the RMS transverse momentum spread of the bunch in the SHINE 3.9 GHz section is similar to that in LCLS-II, which is around 1.3 kV [23] with the voltage less than 5%, the emittance growth caused by HOMs is expected to be small. The E-field distribution of the mode with the maximum transverse voltage ratio is described in Fig. 13b. The mode is an octupole TE-like mode with $R_{\perp}/Q < 10^{-3}\Omega$. In consideration of the above facts, we do not expect dangerous HOMs in the SHINE 3.9 GHz cavity design.

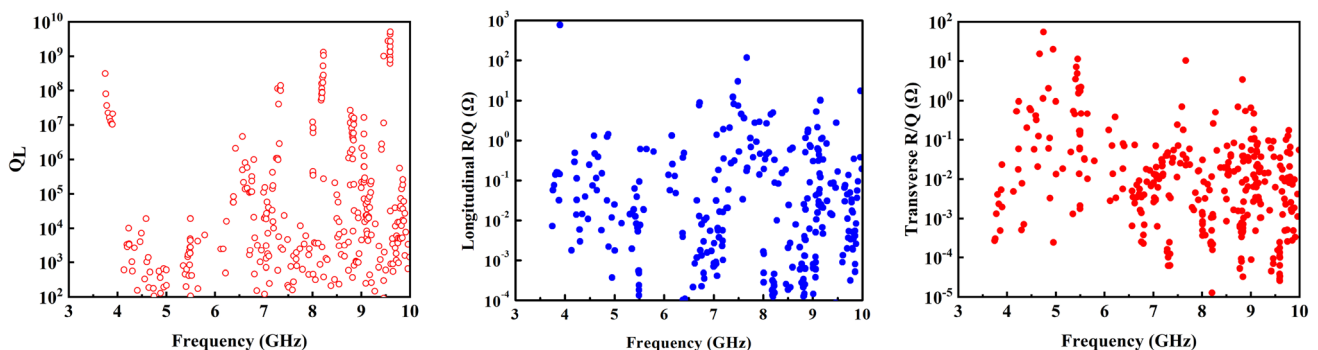


Fig. 11 (Color online) The Q_L , longitudinal R/Q , and transverse R/Q versus frequency of all modes under 10 GHz in SHINE 3.9 GHz cavity

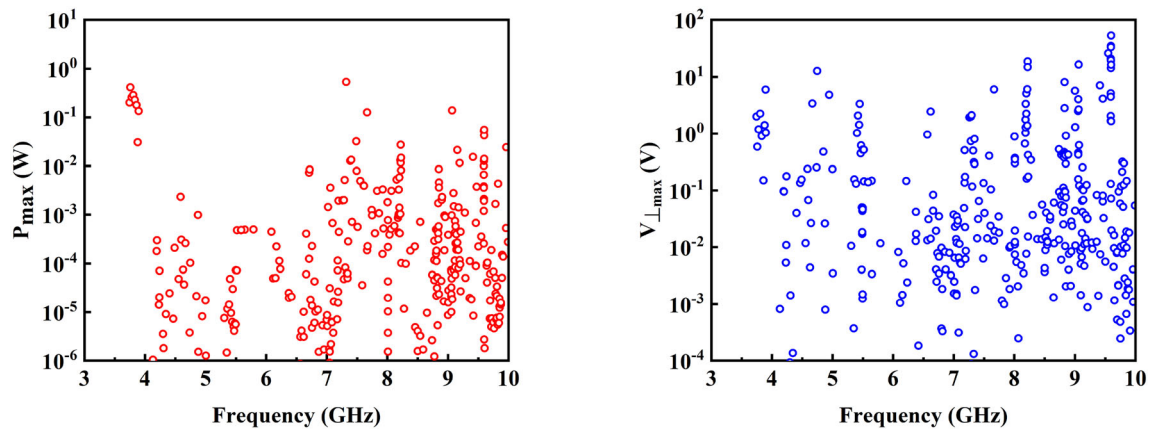


Fig. 12 (Color online) Maximum power loss and transverse voltage of all modes (except accelerating) under 10 GHz in SHINE 3.9 GHz cavity

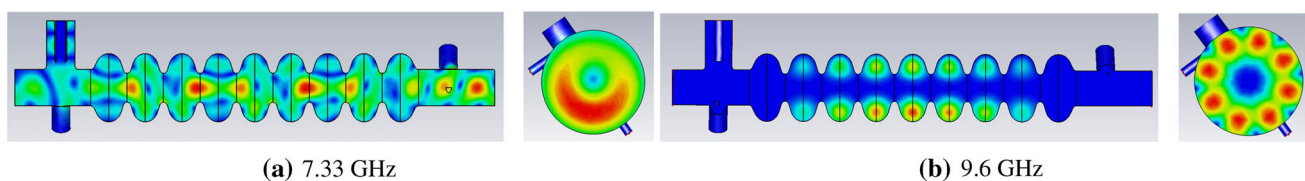


Fig. 13 (Color online) Electric field distribution in two planes of the two modes at 7.33 GHz and 9.6 GHz in SHINE 3.9 GHz cavity

6 Discussion

According to the FNAL studies, multipacting is not an issue in this HOM coupler design [24]. Multipacting did not appear in all the vertical test results of the E-XFEL 3.9 GHz cavities at LASA [9]. Therefore, we do not expect any surprises from multipacting in our cavity design. In this paper, we only describe the HOMs in one 3.9 GHz cavity. Some more HOM studies for the cavity string in a cryomodule are expected to be performed in the near future to assess the full HOM damping. Mechanical analysis of the cavity and the cryogenic design of the helium tank and chimney are underway as well. Figure 14 shows a drawing of the bare SHINE 3.9 GHz cavity.

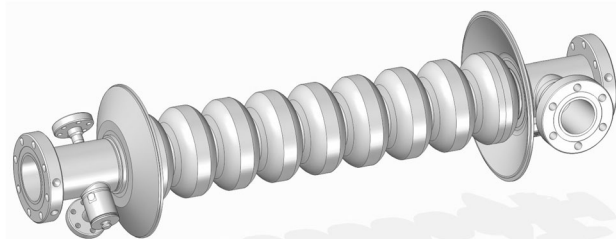


Fig. 14 Bare SHINE 3.9 GHz cavity

7 Conclusion

An optimized RF design for a 3.9 GHz cavity has been proposed for the SHINE project based on the existing E-XFEL and LCLS-II designs. We particularly redesigned the end groups of the cavity with a simple geometry with the aim of improving its performance for CW operation. A systematic study on the cavity RF design has been carried out, including a careful check of potentially dangerous HOMs. The simulation results show that the optimized design meets the SHINE requirements. Based on this design, we plan to fabricate some prototype cavities to verify their performance in the near future.

Acknowledgements The authors would like to thank Paolo Pierini at ESS and Carlo Pagani at INFN-LASA for pre-reviewing the RF design. We are also grateful to Meng Zhang at SARI for discussing the physics parameters in the SHINE Linac and to Hongjuan Zheng at IHEP for discussing the HOM-related issues.

References

1. Z.Y. Zhu, Z.T. Zhao, D. Wang et al., SCLF: an 8-GeV CW SCRF linac-based X-ray FEL facility in Shanghai, in *Proceedings of the FEL2017*, Santa Fe, NM, USA (2017), p. 20. <https://doi.org/10.18429/jacow-fel2017-mop055>
2. Z.T. Zhao, C. Feng, K.Q. Zhang, Two-stage EEHG for coherent hard X-ray generation based on a superconducting linac. *Nucl. Sci. Tech.* **28**, 117 (2017). <https://doi.org/10.1007/s41365-017-0258-z>

3. C. Feng, H.X. Deng, Review of fully coherent free-electron lasers. *Nucl. Sci. Tech.* **29**, 160 (2018). <https://doi.org/10.1007/s41365-018-0490-1>
4. K. Flöttmann, T. Limberg, P. Piot, Generation of Ultrashort Electron Bunches by cancellation of nonlinear distortions in the longitudinal phase space. TESLA-FEL-2001-06 https://flash.desy.de/sites2009/site_vuvfel/content/e403/e1642/e772/e773/infoBoxContent779fel2001-06.pdf
5. N. Solyak, I. Gonin, H. Edwards et al., Development of the third harmonic SC cavity at Fermilab. *Proc. IEEE Particle Accel. Conf.* **2**, 1213–1215 (2003). <https://doi.org/10.1109/pac.2003.1289656>
6. M. Zhang, Linac Requirement. SHINE-AC-SCL-PHY-PR-0001
7. E. Plönjes, B. Faatz, M. Kuhlmann et al., FLASH2: Operation, beamlines, and photon diagnostics. *AIP Conf. Proc.* **1741**, 020008 (2016). <https://doi.org/10.1063/1.4952787>
8. W.F.O. Müller, J. Sekutowicz, R. Wanzenberg, et al., A Design of a 3rd Harmonic Cavity for the TTF 2 Photoinjector. TESLA-FEL 2002-05 https://flash.desy.de/sites2009/site_vuvfel/content/e403/e1642/e750/e751/infoBoxContent754/fel2002-05.pdf
9. P. Pierini, M. Bertucci, A. Bosotti, et al., Fabrication and vertical test experience of the European X-ray Free Electron Laser 3.9 GHz superconducting cavities. *Phys. Rev. Accel. Beams* **20**, 042006 (2017). <https://doi.org/10.1103/PhysRevAccelBeams.20.042006>
10. M. Altarelli, The European X-ray free-electron laser facility in Hamburg. *Nucl. Instrum. Meth. B.* **269**(24), 2845–2849 (2011). <https://doi.org/10.1016/j.nimb.2011.04.034>
11. A. Lunin, I.V. Gonin, T.N. Khabiboulline, et al., Redesign of the End Group in the 3.9 GHz LCLS-II Cavity, in *Proceeding of LINAC2016, East Lansing, MI, USA*, MOPLR007, pp. 145–148, <https://doi.org/10.18429/JACoW-LINAC2016-MOPLR007>
12. T. Khabiboulline, C. Cooper, N. Dhanaraj et al., 3.9 GHz superconducting accelerating 9-cell cavity vertical test results. *IEEE Particle Accel. Conf. (PAC)*. Albuquerque, NM **2007**, 2295–2297 (2007). <https://doi.org/10.1109/PAC.2007.4441228>
13. T. Arkan, P. Bauer, L. Bellantoni, et al., Development of the superconducting 3.9 GHz accelerating cavity at Fermilab. *Proceedings of the 2005 Particle Accelerator Conference*, Knoxville, TN, USA, 2005, pp. 3825–3827. <https://doi.org/10.1109/PAC.2005.1591636>
14. T. Khabiboulline, M. Awida, I. Gonin, et al., Modification of 3rd harmonic cavity for CW operation in LCLS-II accelerator. in *Proceedings of NAPAC2016*, WEPOB27. <http://accelconf.web.cern.ch/napac2016/papers/wepob27.pdf>
15. SUPERFISH, https://laacg.lanl.gov/laacg/services/serv_cod
16. J.F. Chen, M. Moretti, P. Pierini, et al., Improvements of build-cavity code. SRF2015, THPB006, <https://accelconf.web.cern.ch/SRF2015/papers/thpb006.pdf>
17. Buildcavity v1.4.3, <http://www.srf.mil.infn.it/Members/pierini>
18. L. Merminga, J. Delayen, On the optimization of Qext under heavy beam loading and in the presence of microphonics. CEBAF TN-96-022, May 1996. <https://www.jlab.org/uspas11/MISC/Beam%20loading%20TN.pdf>
19. P.P. Gong, Y.B. Zhao, H.T. Hou et al. Front-end frequency conversion module design for harmonic RF system in SSRF. *Nucl. Tech.*, 42: 010101 (2019). (in Chinese) <https://doi.org/10.11889/j.0253-3219.2019.hjs.42.010101>
20. CST-computer Simulation Technology, <http://www.cst.com>
21. A. Lunin, T. Khabiboulline, N. Solyak, et al., Resonant excitation of high order modes in the 3.9 GHz cavity of the Linac Coherent Light Source. *Phys. Rev. Accel. Beams* **21**, 022001 (2018). <https://doi.org/10.1103/PhysRevAccelBeams.21.022001>
22. P. Zhang, N. Baboi, R.M. Jones, Eigenmode simulations of third harmonic superconducting accelerating cavities for FLASH and the European XFEL. [arXiv:1206.2782](https://arxiv.org/abs/1206.2782)
23. P. Emma, J. Frisch, Z. Huang, et al., Linear Accelerator Design For The LCLS-II FEL Facility. in *Proceedings of FEL2014*, THP025. <https://accelconf.web.cern.ch/FEL2014/papers/thp025.pdf>
24. T.N. Khabiboulline, A. Lunin, G.R. Romanov, Multipacting in the LCLS-II 3.9 GHz HOM coupler. TD-17-002. <https://web.fnal.gov/organization/TDNotes/Shared%20Documents/2017%20Tech%20Notes/TD-17-002.pdf>